UT–14–33

Heavy WIMP through Higgs portal at the LHC

Motoi Endo and Yoshitaro Takaesu

Department of Physics, University of Tokyo, Tokyo 113–0033, Japan

arXiv:1407.6882v1 [hep-ph] 25 Jul 2014

Abstract

LHC constraints on Higgs-portal WIMPs are studied. Scalar, vector and anti-symmetric tensor fields are considered. They are assumed to be heavier than a half of the Higgs boson mass. We investigate 8 TeV LHC results on signatures of the vector boson fusion, mono-jet and associated production of the Z boson, which proceed via virtual exchange of the Higgs boson. We show that Higgs-portal interactions of the vector and tensor WIMPs are constrained to be less than 0.43 and 0.16, respectively, while those for the scalar are very weak. Prospects of the 14 TeV LHC are also discussed.

1 Introduction

Although astrophysical and cosmological evidences have established the existence of the dark matter (DM), its nature has not been demystified (see, e.g., Ref. [1] for a review). In particular, DM interactions with standard model (SM) particles have not been identified except for gravitational ones in spite of enormous experimental efforts. They have been limited by direct or indirect DM searches, for instance, by the LUX experiment [2]. Besides, if the DM has sizable couplings with quarks or gluons, it can be discovered or constrained by collider experiments especially at the LHC [3]. In fact, searching for the DM is one of the main targets for the next phase of the LHC.

The collider searches are qualitatively different from the direct and indirect ones for the DM. The latter particularly depends on the relic abundance of the DM as well as its interactions. For a subcomponent of the DM, the signal strength of direct or indirect searches can be suppressed, even if its coupling is strong. In contrast, signal strengths at colliders depend only on interactions. Weakly-interacting massive particles (WIMPs) are searched, irrespective of whether they are dominant components of the DM. They are assumed to be stable and identified as a missing momentum in detectors.

In this letter, we study LHC signatures of stable WIMPs through the Higgs portal, where they interact with the SM particles only via the Higgs boson. They are assumed to be singlet under the SM gauge symmetries. An unbroken Z_2 parity is introduced, where the stability of WIMPs is guaranteed by assigning odd (even) charge to WIMP (SM) particles. We consider scalar, vector and anti-symmetric tensor fields as a candidate of Higgs-portal WIMPs[#1].

Although the Higgs-portal models have been constrained by LHC studies on the Higgs invisible decay, they target WIMPs lighter than a half of the Higgs boson mass [5–7]. In this letter, we study LHC signatures of WIMPs when they are *heavier*. We explore the vector boson fusion (VBF) and Z-boson associated production channels. Besides, WIMPs are produced by gluon fusions via top loops and the intermediate Higgs boson. Such a channel can be identified by using associate productions of a hard jet. Thus, we also investigate the mono-jet signature in light of the current LHC studies [8, 9]. It will be shown that the current LHC results constrain the Higgs-portal interactions of the vector and tensor WIMPs to be less than 0.43 and 0.16, respectively, while those for the scalar is very weak. Prospects of the 14 TeV LHC will also be discussed.

The remaining parts of this work are organized as follows. After introducing the Higgs-portal models in Section 2, the relevant LHC signatures and analysis details are described in Section 3. Results for the 8 TeV LHC constraints are shown in Section 4, while Section 5 is devoted to discussions on prospects for the 14 TeV LHC. Finally, our main conclusion are summarized in Section 6.

[#1] The stability of the tensor WIMP does not always require a new Z_2 symmetry [4].

2 Model

Higgs-portal WIMP models are considered, where WIMP is a scalar, S, vector, V_μ, or anti-symmetric tensor field, $B_{\mu\nu}$[#2]. It generally couples to the Higgs boson via a dimension-four interaction operator. The Lagrangian is generally given as

$$\mathcal{L}_S = \frac{1}{2}\partial^\mu S \partial_\mu S - \frac{1}{2}M_S^2 S^2 - \lambda_S S^4 - c_S \left|H\right|^2 S^2, \tag{2.1a}$$

$$\mathcal{L}_V = -\frac{1}{4}V^{\mu\nu}V_{\mu\nu} + \frac{1}{2}M_V^2 V^\mu V_\mu - \lambda_V (V^\mu V_\mu)^2 + c_V \left|H\right|^2 V^\mu V_\mu, \tag{2.1b}$$

$$\begin{aligned}\mathcal{L}_B = {} & \frac{1}{4}\partial_\lambda B^{\mu\nu}\partial^\lambda B_{\mu\nu} - \frac{1}{2}\partial^\mu B_{\mu\nu}\partial_\rho B^{\rho\nu} - \frac{1}{4}M_B^2 B^{\mu\nu}B_{\mu\nu} \\ & - \lambda_B B_{\mu\nu}B^{\nu\lambda}B_{\lambda\rho}B^{\rho\mu} - c_B \left|H\right|^2 B^{\mu\nu}B_{\mu\nu},\end{aligned} \tag{2.1c}$$

where M_χ, λ_χ and c_χ are the mass parameter, quartic self-coupling and interaction strength between the Higgs boson and WIMP, respectively, for $\chi = S, V, B$. In the LHC analysis, c_χ is set to be a real and positive value without loss of generality. Also, $V_{\mu\nu}$ is a field strength of the vector. After the electroweak symmetry is broken, the WIMP mass receives a correction of $\sim c_\chi v^2$. In the analysis, the physical WIMP mass is represented as m_χ. In this letter, we follow Ref. [4] for the tensor model, where a massive anti-symmetric two-form field is analyzed in the transverse representation as a candidate of the DM. In particular, the wave function becomes

$$\left\langle 0 \left| B_{\mu\nu} \right| b(q,\lambda) \right\rangle = \frac{i}{m_B}\epsilon_{\mu\nu\rho\sigma}\,\varepsilon^\rho(\lambda) q^\sigma, \tag{2.2}$$

for momentum q and helicity λ.

The invisible decay rate of the Higgs boson with a mass m_H is calculated as

$$\Gamma_S(m_H, m_S; c_S) = \frac{c_S^2}{8\pi}\frac{v^2}{m_H}\sqrt{1 - \frac{4m_S^2}{m_H^2}}, \tag{2.3a}$$

$$\Gamma_V(m_H, m_V; c_V) = \frac{c_V^2}{32\pi}\frac{v^2}{m_H}\frac{m_H^4 - 4m_H^2 m_V^2 + 12 m_V^4}{m_V^4}\sqrt{1 - \frac{4m_V^2}{m_H^2}}, \tag{2.3b}$$

$$\Gamma_B(m_H, m_B; c_B) = \frac{c_B^2}{4\pi}\frac{v^2}{m_H}\frac{m_H^4 - 4m_H^2 m_B^2 + 6 m_B^4}{m_B^4}\sqrt{1 - \frac{4m_B^2}{m_H^2}}, \tag{2.3c}$$

where v is the vacuum expectation value of the Higgs field, $v \simeq 246\,\mathrm{GeV}$. It is noticed that the vector and tensor productions are enhanced by m_H^4/m_χ^4, if m_H is much larger than m_χ. For the vector final state, this comes from the longitudinal polarization. On the other hand, in the tensor case the wave function (2.2) is proportional to $\varepsilon^\rho q^\sigma / m_B$ but vanishes

[#2] It is straightforward to apply the following analysis for a fermion WIMP, which interacts with the Higgs boson by a dimension-five operator.

for $\varepsilon^\rho(\lambda) \propto q^\rho$, leading to the similar scaling behavior in high energy as the vector case. Consequently, the Higgs invisible decay rate becomes large especially for the vector and tensor WIMPs.

3 LHC Signatures

In this section we discuss LHC signatures for the Higgs-portal models described in the previous section.

Higgs invisible decay signals are definitive probes for the Higgs-portal interactions. ATLAS and CMS collaborations have put limits on the branching fraction of the Higgs invisible decay ($\mathrm{BR}_{\mathrm{inv}}$) based on VBF and ZH associated production processes [5, 6]. Those constraints can be reinterpreted for bounds on the heavy Higgs-portal WIMP models, where off-shell Higgs bosons intermediate between the SM particles and WIMPs. Besides, new physics searches via mono-jet [8,9], mono-Z [10,11] and mono-W [10,12] signatures can also be a way to investigate Higgs-portal models.

In the following, we explain details of our VBF, mono-jet and mono-Z analyses for constraints on the heavy Higgs-portal models. On the other hand, since the currently available LHC results for the ZH [5, 6] and mono-W [10, 12] signatures are based on the template-based analyses (i.e., depending on kinematical distributions of decay products), it is not straightforward to reinterpret them for the constraints on the Higgs-portal models. We do not investigate these channels in this study.

3.1 Vector Boson Fusion

We briefly explain the analysis details for VBF constraints on the Higgs-portal models. WIMP-pair productions are intermediated by the Higgs boson, H^*, as

$$pp \to H^* + jj \to \chi\chi + jj, \tag{3.1}$$

where the Higgs is off-shell when the WIMP is heavier than a half of the Higgs boson mass. Its cross section can be expressed as

$$\sigma_{\chi\chi}(m_\chi, c_\chi) = \int_{4m_\chi^2}^{\infty} \frac{d\tilde{s}}{2\pi}\, \sigma_H(m_H = \sqrt{\tilde{s}}) \frac{2\sqrt{\tilde{s}}}{(\tilde{s} - m_h^2)^2 + \Gamma_h^2 m_h^2}\, \Gamma_\chi(\sqrt{\tilde{s}}, m_\chi; c_\chi), \tag{3.2}$$

where $\tilde{s}$ is the invariant mass squared of the $\chi\chi$ system, and $\Gamma_h = 4.21\,\mathrm{MeV}$ is the total decay width of the Higgs boson at the mass, $m_h = 125\,\mathrm{GeV}$ [13]. The cross section consists of the following three parts: i) the production cross section of the Higgs boson, σ_H, at a hypothetical mass of the Higgs boson, $m_H = \sqrt{\tilde{s}}$, ii) the Higgs boson propagator at the four momentum squared $\tilde{s}$, and iii) the decay width of the Higgs boson into a pair of WIMPs, Γ_χ, provided in Eq. (2.3), where the Higgs mass is supposed to be $m_H = \sqrt{\tilde{s}}$. It should be noted that the hypothetical Higgs boson mass m_H is not equal to the SM Higgs boson mass

m_h. Higgs production cross sections, σ_H, depend on Higgs production processes, e.g., Higgs plus one jet, VBF and ZH associated production, while the Higgs propagator and Γ_χ are universal for all the production processes. Thus, our main concern in evaluating a WIMP-pair production cross section is the calculation of the corresponding Higgs production cross section for various Higgs masses.

The cross section, σ_H, for the VBF process is calculated with the HAWKv2.0 package [14, 15] at the next-to-leading order (NLO), including QCD and EW corrections. We impose the following kinematical cuts based on the CMS VBF analysis [6]:

$$\begin{aligned} & p_{Tj_{1(2)}} > 50\,\mathrm{GeV}, \;\; |\eta_{j_{1(2)}}| < 4.7, \\ & \eta_{j_1}\eta_{j_2} < 0, \;\; \Delta\eta_{jj} > 4.2, \;\; |\Delta\phi_{jj}| < 1, \;\; M_{jj} > 1100\,\mathrm{GeV}, \\ & p_{TH} > 130\,\mathrm{GeV}, \end{aligned} \tag{3.3}$$

where $p_{Tj_{1(2)}}$ and $\eta_{j_{1(2)}}$ are the transverse momentum and pseudo-rapidity of the first (second) leading jet, respectively. Also, $\Delta\eta_{jj}, \Delta\phi_{jj}$ and M_{jj} are the rapidity difference, azimuthal-angle difference and invariant mass of the two leading jets, respectively. Since the missing momentum arises solely from the Higgs invisible decay in our simulation, the Higgs transverse momentum, p_{TH}, is equal to the missing transverse momentum, $\not{p}_T$. The CTEQ6L1 parton distribution function (PDF) set [16] is used with the factorization/renormalization scale equal to $(m_H^2 + p_{TH\mathrm{cut}}^2)^{1/2}$, where $p_{TH\mathrm{cut}}$ is the Higgs p_T cut. The following analysis is based on the parton level calculation, and effects of parton shower, hadronization and detector simulation are neglected. Besides, we assume 100% trigger and reconstruction efficiencies, supported by their sufficiently high performance [6]. Also HAWK is modified to implement the $\Delta\phi_{jj}$ cut.

The CMS collaboration has reported that the observed 95% confidence level (CL) upper bound on $\mathrm{BR}_{\mathrm{inv}}$ is 0.65 for the SM Higgs boson with $m_h = 125\,\mathrm{GeV}$, where the upper bound on the signal event number is $210 \times 0.65 \simeq 137$ for the integrated luminosity ($\mathcal{L}$) of $19.5\,\mathrm{fb}^{-1}$ at $\sqrt{s} = 8\,\mathrm{TeV}$ [6]. If we require the VBF Higgs production cross section times the invisible decay branching fraction, $\sigma_H(m_H) \times \mathrm{BR}_{\mathrm{inv}}$, to be smaller than the CMS bound, $\sigma = 210 \times 0.65/19.5\,\mathrm{fb}^{-1} \simeq 7\,\mathrm{fb}$, we can reproduce the CMS upper bound on $\mathrm{BR}_{\mathrm{inv}}$ as a function of the Higgs mass (Fig. 8 in Ref. [6]) within the 1σ level of the experimental uncertainty. Our bound is stronger than that of CMS. The difference may originate in theoretical uncertainties from PDF and factorization/renormalization scales as well as the effects of parton shower, hadronization and detector smearing including the trigger and reconstruction efficiencies, which are neglected in our analysis.

The WIMP production cross section, $\sigma_{\chi\chi}$, is calculated from Eqs. (3.2). Contributions of lower $\tilde{s}$ dominates the integration. The 95% CL upper bound on the Higgs-portal coupling, c_χ, is obtained by requiring the expected event number from the WIMP production process to be less than the CMS limit on the signal excess, 137 events.

3.2 Mono jet

Next we explain the analysis details for the mono-jet constraints on the Higgs-portal models. The WIMP production process contributing to the mono-jet signal is

$$pp \to H^* + j \to \chi\chi + j, \tag{3.4}$$

where j denotes an associated jet, and the intermediate Higgs is off-shell when the WIMP is heavier than a half of the Higgs boson mass.

As in the VBF analysis in the previous subsection, the WIMP-pair production cross section is expressed by Eq. (3.2). Here, the Higgs production cross section, σ_H, corresponds to that of the Higgs plus one hard jet process at a hypothetical Higgs mass, $m_H = \sqrt{\tilde{s}}$. The production proceeds mainly via top quark loops. When either the Higgs boson mass or the jet transverse momentum exceeds twice the top quark mass, $1/m_t$ expansion of the top loop function breaks down, and the finite m_t effects must be taken into account. This is the case when a Higgs-portal WIMP is heavy. The leading order (LO) cross section of the process has been evaluated with the finite top mass [17]. However, the NLO cross section is known only in the infinite m_t limit to the best of our knowledge. Therefore, we take account of the finite m_t effect at the LO level and include the NLO corrections approximately by a K-factor, defined as the ratio of the NLO and LO cross sections in the infinite m_t limit as

$$\sigma_H^{\rm NLO} \simeq \sigma^{\rm LO}_{pp\to Hj}(m_t) \times K, \tag{3.5}$$

$$K = \frac{\sigma^{\rm NLO}_{pp\to Hj}(m_t = \infty)}{\sigma^{\rm LO}_{pp\to Hj}(m_t = \infty)}, \tag{3.6}$$

where the top quark mass is taken to be $m_t = 173\,\text{GeV}$. This procedure should involve potentially large uncertainties mainly due to the breakdown of the infinite m_t approximation. Therefore, it is desirable to calculate finite m_t corrections to the NLO cross section.

The CMS collaboration has reported the most severe limit on the mono-jet production cross section by using the $19.5\,\text{fb}^{-1}$ dataset at $\sqrt{s} = 8\,\text{TeV}$ [9], while the ATLAS collaboration puts a weaker limit based on the $\mathcal{L} = 10.5\,\text{fb}^{-1}$ dataset [8]. We follow the CMS analysis [9] and impose the kinematical cut condition,

$$\begin{aligned} &p_{Tj_1} > 110\,\text{GeV},\ |\eta_{j_1}| < 2.4, \\ &p_{TH} > 450\,\text{GeV}, \end{aligned} \tag{3.7}$$

where p_{Tj_1} and η_{j_1} are the transverse momentum and pseudo-rapidity of the highest p_T jet, respectively, and p_{TH} is the transverse momentum of the Higgs boson. The p_{TH} cut is related to the $\not{p}_T$ cut since the Higgs boson decays invisibly to WIMPs. The above p_{TH} cut condition is chosen to give the most stringent limit on the Higgs-portal interactions, based on the CMS analysis [9]. In our analysis, the cut conditions, Eq. (3.7), are imposed on $\sigma^{\rm LO}_{pp\to Hj}(m_t)$, whereas in the evaluation of the K-factor we take the p_{TH} cut as low as $m_H/2$[#3]

[#3] This choice of the p_{TH} cut avoids large $\log(m_H/p_{TH})$ corrections (see Ref. [18]).

instead of taking 450 GeV in order to tame the large deviation from the finite m_t result. Here, we suppose that the K-factor does not change significantly with p_{TH} (cf. Ref. [19]). We use the modified MCFMv6.8 package [20], where we implement the p_{TH} cut, to calculate the cross section. The LO (NLO) MSTW2008 PDF set [21] is used for the LO (NLO) cross section calculations with the renormalization/factorization scale of $(m_H^2 + p_{TH\,\mathrm{cut}}^2)^{1/2}$. It is mentioned that the NLO corrections may be overestimated, since we do not impose the veto on the secondary jet from the NLO real emission corrections unlike the CMS analysis [6].

For $p_{TH} > 450\,\mathrm{GeV}$, which is equivalent to $\not{p}_T > 450\,\mathrm{GeV}$ at LO, the observed CMS upper bound on the signal event number is 157 at 95% CL after imposing the cuts at $\sqrt{s} = 8\,\mathrm{TeV}$ and $\mathcal{L} = 19.5\,\mathrm{fb}^{-1}$ [6]. Thus, the production cross section of the mono-jet signal is required to be smaller than $\sigma = 157/19.5\,\mathrm{fb}^{-1} \simeq 8.1\,\mathrm{fb}$ at 95% CL. This CMS result constrains the Higgs-portal coupling, c_χ, in the similar way as the VBF case in the previous section.

3.3 Mono Z

The WIMP production process contributing to the mono-Z signal is

$$pp \to H^* + Z \to \chi\chi + Z. \tag{3.8}$$

The ATLAS collaboration has reported dark matter searches with hadronically decaying mono-W/Z and leptonically decaying mono-Z channels with $\mathcal{L} = 20.3\,\mathrm{fb}^{-1}$ at $\sqrt{s} = 8\,\mathrm{TeV}$ [10, 11][#4]. The most severe limit on the mono-Z production cross section is set by the leptonic mode. We follow the leptonic mode analysis [11] and impose the kinematical cut condition,

$$\begin{aligned} &p_{Tl} > 20\,\mathrm{GeV},\ |\eta_l| < 2.5, \\ &76\,\mathrm{GeV} < m_{ll} < 106\,\mathrm{GeV}, \\ &|\Delta\eta_{ll}| < 2.5, \\ &p_{TH} > 150\,\mathrm{GeV}, \end{aligned} \tag{3.9}$$

where p_{Tl} and η_l are lepton transverse momentum and pseudo-rapidity ($l = e, \mu$), and m_{ll} and $\Delta\eta_{ll}$ are the invariant mass and the difference of the pseudo-rapidities of the two leading leptons, respectively. The above p_{TH} cut condition is chosen to give the most stringent limit on the Higgs-portal interactions, based on the ATLAS analysis [11]. We use the HAWKv2.0 package [14, 15], where we have implemented the $\Delta\eta_{ll}$ cut, and calculate the cross section of the Higgs production process, $pp \to H^*Z$, including NLO QCD and EW contributions. The CTEQ6M PDF set [16] is used with the renormalization/factorization scale of $m_H + m_Z$. It is mentioned that we do not impose jet vetoes unlike the ATLAS analysis [11].

For $\not{p}_T > 150\,\mathrm{GeV}$, which is equivalent to $p_{TH} > 150\,\mathrm{GeV}$ at LO, the observed ATLAS upper bound on the production cross section is 2.7 fb^{-1} at 95% CL. This result constrains the Higgs-portal coupling, c_χ, in a similar way as the VBF and mono-jet cases.

[#4] Signal topologies of the ZH production processes [5, 6], where the Higgs boson is supposed to decay invisibly, are the same as those of the mono-Z production processes [10, 11]. However, Refs. [5, 6] uses the template-based analysis, and we do not consider them.

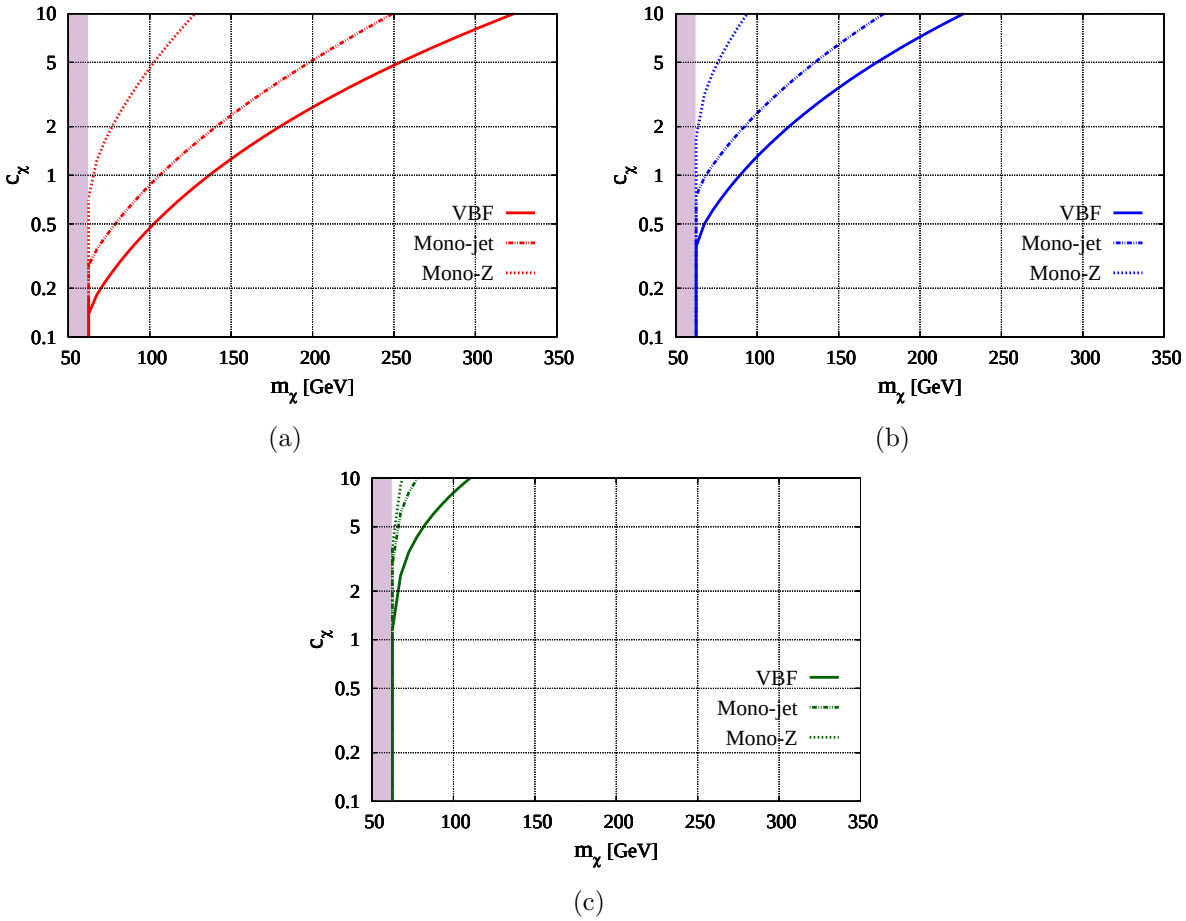

(a) (b)

(c)

Figure 1: The 8 TeV LHC constraints on the tensor (a), vector (b) and scalar (c) Higgs-portal couplings, c_χ, as a function of the WIMP mass m_χ. The solid, dot-dashed and dotted curves correspond to the 95% CL upper bounds based on the VBF, mono-jet and mono-Z data [6, 9, 11]. The shaded area for $m_\chi < m_h/2$ is excluded by the Higgs invisible decay analysis [5, 6].

4 Limits on the Higgs-portal models

In this section we present the constraints on the Higgs-portal scalar, vector and tensor productions by the VBF, mono-jet and mono-Z studies at the 8 TeV LHC.

In Figs. 1 we show the constraints on the Higgs-portal coupling constant, c_χ, defined in Eqs. (2.1) as a function of the dark matter mass, m_χ. The figures (a), (b) and (c) show the 95% CL upper bounds for the tensor, vector and scalar cases, respectively, based on the VBF (solid), mono-jet (dot-dashed) and mono-Z (dotted) analyses [6, 9]. There is a rapid change in the bounds around $m_\chi = m_h/2\,(\simeq 62.5\,\text{GeV})$ due to the on-shell Higgs pole. The strong constraint on the Higgs invisible decay branching fraction for $m_\chi < m_h/2$ (the shaded area)

is invalid for $m_\chi > m_h/2$.

The VBF result puts about twice stronger bounds than the mono-jet ones, while the mono-Z bound is weaker than them. This is because the VBF signals are clean against backgrounds, while the cross section of the mono-Z productions is too small. It is found that the VBF process constrains the couplings of the tensor, vector and scalar to be smaller than 0.16, 0.43 and 2.0 at $m_\chi = 65\,\mathrm{GeV}$, respectively. The bounds becomes weaker for larger m_χ since the WIMP production cross section is proportional to $1/m_\chi^4$. However, for the vector and tensor cases, this reduction of the cross section is relaxed due to the m_H^4/m_χ^4 enhancement with respect to the scalar case in the large WIMP-pair invariant mass (m_H) region, as discussed in Sec. 2. Especially, the tensor coupling receives the most stringent constraint in the all range of the WIMP mass, which is stronger than the vector case by a factor of ~ 3. If the coupling constant becomes as large as $c_\lambda \sim 4\pi \sim 10$, the perturbative description of Eq. (3.2) breaks down. Thus, the VBF, mono-jet and mono-Z bounds work only below $m_\chi \sim 320$, 250 and 130 GeV for the tensor interaction, while the limit is 220, 170 and 90 GeV and 110, 80 and 70 GeV for the vector and scalar ones, respectively.

Although these collider limits are weaker than that from the relic abundance and direct detection of the DM [4, 22], we stress that the collider limit is valid even if the hidden sector particle of interest is not the dominant component of the DM.

5 Future Prospects

In this section, we discuss future prospects of the sensitivity to the Higgs-portal models at the 14 TeV LHC.

5.1 Mono-jet prospects

In order to discuss future prospects, we need to evaluate the signal event number and backgrounds. First, let us estimate expected backgrounds and upper bounds on the signal excess with the following assumptions:

- Backgrounds event number (N_{BG}) is scaled by the integrated luminosity, $\mathcal{L}$, and the parton luminosity function, $L(\hat{s})$, at a typical center-of-mass energy scale of partonic collisions, $\sqrt{\hat{s}}$, for the background process. Here the parton luminosity function is defined as

$$L(\hat{s}) \equiv \int_{-\ln(1/\sqrt{\tau})}^{\ln(1/\sqrt{\tau})} dy\, f_a(\sqrt{\tau}e^y, Q) f_b(\sqrt{\tau}e^{-y}, Q), \quad \tau = \frac{\hat{s}}{s}, \tag{5.1}$$

  where $f_i(x, Q)$ is a PDF for an incoming parton flavor i with a longitudinal momentum fraction x at a factorization scale Q. Thus, from the experimental result at $\sqrt{s} = 8\,\mathrm{TeV}$, N_{BG} at $\sqrt{s} = 14\,\mathrm{TeV}$ is deduced as

$$N_{\mathrm{BG}}^{14\,\mathrm{TeV}} = \frac{\mathcal{L}^{14\,\mathrm{TeV}}}{\mathcal{L}^{8\,\mathrm{TeV}}} \frac{L^{14\,\mathrm{TeV}}(\hat{s})}{L^{8\,\mathrm{TeV}}(\hat{s})} N_{\mathrm{BG}}^{8\,\mathrm{TeV}}, \tag{5.2}$$

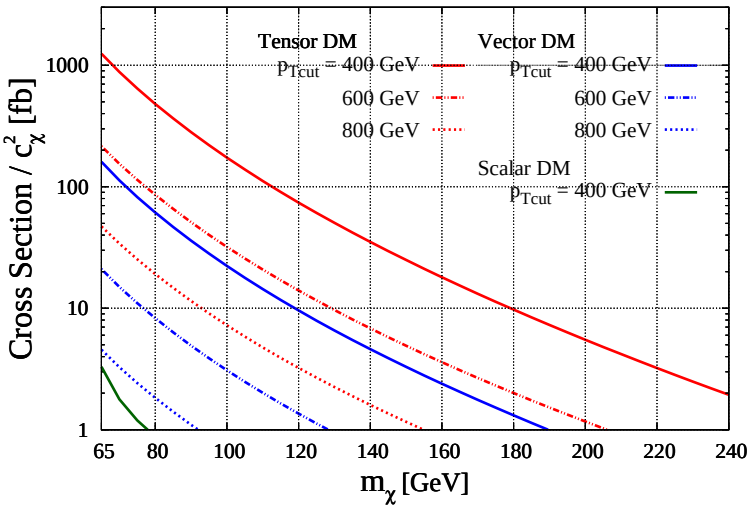

Figure 2: The cross sections of the tensor, vector and scalar WIMP-pair productions associated with one jet at the 14 TeV LHC as functions of the WIMP mass. The vertical axis is rescaled by the Higgs-portal coupling squared. The red, blue and green curves are for the tensor, vector and scalar cases, respectively, with the p_{TH} cut of 400 (solid), 600 (dot-dashed) and 800 GeV (dotted).

For the mono-jet process, the background is dominated by $Z+$jets productions. Then, the parton luminosity function is calculated for $q\bar{q}$ initial states ($q = u, d, s, c, b$) with $Q = \sqrt{\hat{s}} = \sqrt{m_Z^2 + \not{p}_{T\rm cut}^2} + \not{p}_{T\rm cut}$, where $\not{p}_{T\rm cut}$ is the missing p_T cut.

- The relative systematic uncertainty is the same level as those at the 8 TeV LHC,

$$\frac{\sigma_{\rm sys}^{14\,\rm TeV}}{N_{\rm BG}^{14\,\rm TeV}} = \frac{\sigma_{\rm sys}^{8\,\rm TeV}}{N_{\rm BG}^{8\,\rm TeV}}, \tag{5.3}$$

while the statistical uncertainty is scaled as

$$\frac{\sigma_{\rm stat}^{14\,\rm TeV}}{\sqrt{N_{\rm BG}^{14\,\rm TeV}}} = \frac{\sigma_{\rm stat}^{8\,\rm TeV}}{\sqrt{N_{\rm BG}^{8\,\rm TeV}}}. \tag{5.4}$$

The total uncertainty $\sigma_{\rm tot}$ is estimated by adding these uncertainties in quadrature.

- Expected upper bound on the signal excess is estimated as

$$N_{\rm sig} < 2\,\sigma_{\rm tot}. \tag{5.5}$$

Next, in Fig. 2 we show the cross sections of the jet-associated WIMP-pair production process, $pp \to \chi\chi j$, at the 14 TeV LHC as functions of the WIMP mass. Here, the vertical axis

is rescaled by the Higgs-portal coupling squared, c_χ^2, since the cross section is proportional to c_χ^2. The red, blue and green curves are for the tensor, vector and scalar cases, respectively. The cut conditions are supposed to be the same as the 8 TeV analysis (see Eq. (3.7)), but the p_{TH} cut is taken as 400 (solid), 600 (dot-dashed) and 800 GeV (dotted).

The estimated upper bound becomes $\sim$ 4900 events for the p_{TH} cut of 400 GeV at $\mathcal{L} = 100\text{fb}^{-1}$, based on the CMS mono-jet result at the 8 TeV LHC [9]. On the other hand, the signal event number for the tensor production with $m_\chi = 65$ GeV is estimated to be ~ 1200 for $c_\chi = 0.1$. Thus, if the p_{TH} cut of 400 GeV is still applicable at the 14 TeV LHC, the Higgs-portal tensor model can be probed for a coupling as small as ~ 0.2 at $m_\chi = 65$ GeV and $\mathcal{L} = 100\,\text{fb}^{-1}$. Expected signal event number decreases rapidly for heavier WIMPs. The signal becomes about 10 events for $m_\chi = 180$ GeV with $c_\chi = 0.1$ at $\mathcal{L} = 100\,\text{fb}^{-1}$.

For $p_{TH} > 550$ GeV, the expected signal events and the expected upper bound on the signal excess become ~ 300 (for $c_\chi = 0.1$) and ~ 2000 events at $\mathcal{L} = 100\,\text{fb}^{-1}$, respectively. This leads to a weaker limit on the Higgs-portal coupling as ~ 0.3. Thus, harder p_{TH} cut may degrade the sensitivity to the Higgs-portal couplings for the mono-jet channel at the 14 TeV LHC. Dedicated studies on the backgrounds and cut conditions are needed for a definitive conclusion.

The sensitivities to the vector and scalar models are weaker than the tensor one. The production cross section of the vector is smaller by a factor than that of the tensor, and the tensor result can be reinterpreted to the vector model straightforwardly. On the other hand, the mono-jet channel will be hopeless to probe the Higgs-portal scalar model with a coupling of ~ 0.1 even at the 14 TeV LHC because of the too small production cross section.

5.2 Mono-Z prospects

Future prospects at the 14 TeV LHC for the mono-Z channel is discussed along the lines of the previous subsection for the mono-jet channel. Expected backgrounds and upper bounds on the signal excess are estimated in a similar way, but the dominant background is ZZ productions. Then, the parton luminosity function is calculated for $q\bar{q}$ initial states ($q = u, d, s, c, b$) with $Q = \sqrt{\hat{s}} = 2\sqrt{m_Z^2 + \not{p}_{T\text{cut}}^2}$.

In Fig. 3, we show the cross sections of the Z-associated WIMP-pair production process, $pp \to \chi\chi Z$, at the 14 TeV LHC as functions of the WIMP mass. The red, blue and green curves show the cross sections for the tensor, vector and scalar cases, respectively. Here, the cut conditions are supposed to be the same as the 8 TeV analysis, Eq. (3.9), but the p_{TH} cut is set as 250 (solid), 350 (dot-dashed) or 450 GeV (dotted). The event number of the tensor production with $m_\chi = 65$ GeV is estimated to be ~ 7 events for $c_\chi = 0.1$ and $p_{TH} > 450$ GeV at $\mathcal{L} = 100\,\text{fb}^{-1}$, while the expected upper bound on the signal excess for this integrated luminosity is ~ 15 events, deduced from the ATLAS mono-Z result at the 8 TeV LHC [11]. Thus, if the p_{TH} cut of 450 GeV is applicable at the 14 TeV LHC, the Higgs-portal tensor model can be probed for a coupling as small as ~ 0.15 at $m_\chi = 65$ GeV and $\mathcal{L} = 100\,\text{fb}^{-1}$. It is mentioned that the backgrounds are expected to be suppressed more efficiently by adopting harder p_{TH} cut in the mono-Z channel at the 14 TeV LHC. This

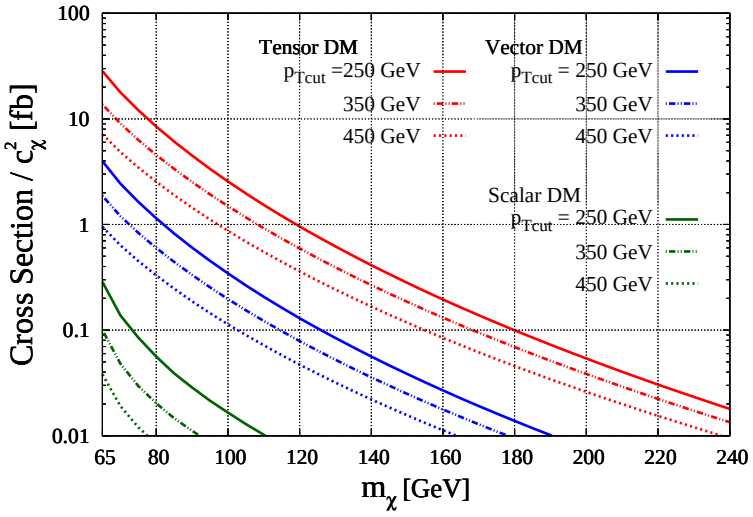

Figure 3: The cross sections of the tensor, vector and scalar WIMP-pair productions associated with a Z boson at the 14 TeV LHC as functions of the WIMP mass. The vertical axis is rescaled by the Higgs-portal coupling squared. The red, blue and green curves are for the tensor, vector and scalar cases, respectively, with the p_{TH} cut of 250 (solid), 350 (dot-dashed) and 450 GeV (dotted).

contrasts sharply with the mono-jet case.

The mono-Z sensitivities to the vector model are weaker than the tensor case. On the other hand, the mono-Z channel will be hopeless to probe the scalar model with a coupling of ~ 0.1 even in the 14 TeV LHC as the mono-jet channel.

5.3 VBF prospects

Let us turn to the VBF process. Future prospects of the Higgs invisible decay branching fraction for the process have been discussed in Ref. [23]. The current upper bound is $\mathrm{BR}_{\mathrm{inv}} < 0.65$ for $m_h = 125\,\mathrm{GeV}$, and the sensitivity is expected to be $\mathrm{BR}_{\mathrm{inv}} \sim 0.17$ for $\sqrt{s} = 14\,\mathrm{TeV}$ and $\mathcal{L} = 100\,\mathrm{fb}^{-1}$. Thus, the limit on $\sigma \times \mathrm{BR}_{\mathrm{inv}}$ will be improved by a factor of 3.8 for $m_h = 125\,\mathrm{GeV}$. If this factor is assumed to be independent of the Higgs boson mass and the kinematical distributions, the limit on the Higgs-portal WIMP coupling, c_χ^{lim}, is expected to be improved by a factor of ~ 2, since the WIMP production cross section, Eq. (3.2), is proportional to c_χ^2. Therefore, the expected limit is estimated to be $c_\chi^{\mathrm{lim}} \sim 0.08$, 0.2 and 1.0 for the tensor, vector and scalar cases, respectively, at $m_\chi = 65\,\mathrm{GeV}$. It should be noted that careful background estimations with reliable detector simulations are required to derive more realistic conclusions on 14 TeV prospects for the Higgs-portal interactions.[#5]

[#5] The background simulation in the VBF analysis [23] seems to discard some contributions such as those due to pileup effects. The signal significance may be degraded especially when the luminosity is large.

6 Conclusion

We discussed the LHC constraints on the several Higgs-portal WIMP models at the LHC. WIMPs are assumed to be scalar, vector and anti-symmetric tensor fields. In particular, we considered their masses heavier than a half of the Higgs boson mass, where LHC analyses have been rarely performed. We found that the current LHC data excludes the models with the Higgs-portal couplings larger than 0.16 (tensor), 0.43 (vector) and 2.0 (scalar) for $m_\chi = 65\,\mathrm{GeV}$, while these constraints become weaker for heavier WIMPs. The tensor and vector Higgs-portal couplings receive stronger limits than the scalar one especially when WIMPs are heavy. The tensor WIMP coupling is constrained most strongly for any WIMP masses. On the other hand, for $m_\chi > 320$ (tensor), 220 (vector) and 110 GeV (scalar), our analyses cannot be applied since the perturbative calculations break down.

We also discussed the prospects for 14 TeV LHC sensitivities to the Higgs-portal interactions. For the mono-jet and mono-Z processes, we evaluated the production cross sections of the Higgs-portal WIMPs with several cut conditions. It was shown that for mono-jet (mono-Z) process more than 1000 (5) events could be produced for the tensor case with $c_\chi = 0.1$ at $\mathcal{L} = 100\,\mathrm{fb}^{-1}$ for $p_{TH} > 400\,(450)\,\mathrm{GeV}$. Although it is difficult to simulate the backgrounds and to estimate the signal significance reliably, we roughly estimated the 14 TeV LHC reach for the Higgs-portal couplings by deducing the upper limits on the signal excesses based on the 8 TeV LHC results. It is found that both mono-jet and mono-Z channels will improve their limits, though this improvement depends on the missing p_T cut condition. The mono-jet channel may prefer the current level cut, while the harder cut will be helpful for the mono-Z channel. It would be still challenging to constrain the scalar WIMP effectively in the $m_\chi > m_H/2$ region even for the 14 TeV LHC. Besides, the Higgs invisible decay channel is expected to be studied accurately by the VBF signal. Then, we may expect a factor of two improvement of the coupling limits at $\mathcal{L} = 100\,\mathrm{fb}^{-1}$. Dedicated studies on realistic estimations of the backgrounds and detector effects are needed for further discussions.

As discussed in this letter, the LHC can probe WIMPs through the Higgs portal not only when they are lighter than a half of the Higgs boson mass but also if they are heavier. Therefore, the LHC will be useful in searching for the Higgs-portal models for wider cases than had been expected.

Acknowledgements

This work was supported by JSPS KAKENHI Grant No. 23740172 (M.E.) and No. 60322997 (Y.T.).

References

[1] G. Bertone, D. Hooper and J. Silk, Phys. Rept. **405**, 279 (2005) [hep-ph/0404175].

[2] D. S. Akerib *et al.* [LUX Collaboration], Phys. Rev. Lett. **112**, 091303 (2014) [arXiv:1310.8214 [astro-ph.CO]].

[3] O. J. P. Eboli and D. Zeppenfeld, Phys. Lett. B **495**, 147 (2000) [hep-ph/0009158].

[4] O. Cata and A. Ibarra, arXiv:1404.0432 [hep-ph].

[5] G. Aad *et al.* [ATLAS Collaboration], Phys. Rev. Lett. **112**, 201802 (2014) [arXiv:1402.3244 [hep-ex]].

[6] S. Chatrchyan *et al.* [CMS Collaboration], arXiv:1404.1344 [hep-ex].

[7] G. Belanger, B. Dumont, U. Ellwanger, J. F. Gunion and S. Kraml, Phys. Lett. B **723**, 340 (2013) [arXiv:1302.5694 [hep-ph]].

[8] [ATLAS Collaboration], ATLAS-CONF-2012-147.

[9] [CMS Collaboration], CMS-PAS-EXO-12-048.

[10] G. Aad *et al.* [ATLAS Collaboration], Phys. Rev. Lett. **112**, 041802 (2014) [arXiv:1309.4017 [hep-ex]].

[11] G. Aad *et al.* [ATLAS Collaboration], arXiv:1404.0051 [hep-ex].

[12] CMS Collaboration [CMS Collaboration], CMS-PAS-EXO-13-004.

[13] S. Heinemeyer *et al.* [LHC Higgs Cross Section Working Group Collaboration], arXiv:1307.1347 [hep-ph].

[14] A. Denner, S. Dittmaier, S. Kallweit and A. Muck, JHEP **1203**, 075 (2012) [arXiv:1112.5142 [hep-ph]].

[15] http://omnibus.uni-freiburg.de/∼sd565/programs/hawk/hawk.html

[16] J. Pumplin, D. R. Stump, J. Huston, H. L. Lai, P. M. Nadolsky and W. K. Tung, JHEP **0207**, 012 (2002) [hep-ph/0201195].

[17] R. K. Ellis, I. Hinchliffe, M. Soldate and J. J. van der Bij, Nucl. Phys. B **297**, 221 (1988).

[18] R. P. Kauffman, Phys. Rev. D **45**, 1512 (1992).

[19] D. de Florian, M. Grazzini and Z. Kunszt, Phys. Rev. Lett. **82**, 5209 (1999) [hep-ph/9902483].

[20] E. L. Berger and J. M. Campbell, Phys. Rev. D **70**, 073011 (2004) [hep-ph/0403194], J. M. Campbell, R. K. Ellis and C. Williams, MCFM web page http://mcfm.fnal.gov

[21] A. D. Martin, W. J. Stirling, R. S. Thorne and G. Watt, Eur. Phys. J. C **63**, 189 (2009) [arXiv:0901.0002 [hep-ph]].

[22] S. Kanemura, S. Matsumoto, T. Nabeshima and N. Okada, Phys. Rev. D **82**, 055026 (2010) [arXiv:1005.5651 [hep-ph]].

[23] D. Ghosh, R. Godbole, M. Guchait, K. Mohan and D. Sengupta, Phys. Lett. B **725**, no. issue, 344 (2013) [arXiv:1211.7015 [hep-ph]].